Foster, A. S.; Pakarinen, O.H.; Airaksinen, J.M.; Gale, J.D.; Nieminen, R. M.

Simulating atomic force microscopy imaging of the ideal and defected TiO_2 (110) surface

Published in:
Physical Review B

DOI:
10.1103/PhysRevB.68.195410

Published: 01/01/2003

Document Version
Publisher's PDF, also known as Version of record

Simulating atomic force microscopy imaging of the ideal and defected TiO_2 (110) surface

A. S. Foster,[1,*] O. H. Pakarinen,[1] J. M. Airaksinen,[1] J. D. Gale,[2] and R. M. Nieminen[1]
[1]*Laboratory of Physics, Helsinki University of Technology, P.O. Box 1100, 02015 Helsinki, Finland*
[2]*Department of Chemistry, Imperial College London, South Kensington SW7 2AZ, United Kingdom*
(Received 14 May 2003; revised manuscript received 20 August 2003; published 18 November 2003)

In this study we simulate noncontact atomic force microscopy imaging of the TiO_2 (110) surface using first-principles and atomistic methods. We use three different tip models to investigate the tip-surface interaction on the ideal surface, and find that agreement with experiment is found for either a silicon tip or a tip with a net positive electrostatic potential from the apex. Both predict bright contrast over the bridging oxygen rows. We then study the interaction of this tip with a bridging oxygen vacancy on the surface, and find that the much weaker interaction observed would result in vacancies appearing as dark contrast along the bright rows in images.

DOI: 10.1103/PhysRevB.68.195410 PACS number(s): 68.37.Ps, 68.47.Gh, 07.05.Tp, 61.72.Ji

I. INTRODUCTION

The importance of titanium dioxide (TiO_2) in a wide variety of applications, from photo-catalysis to biomedical implants,[1–3] has led to a considerable research effort to understand its properties. In most of these applications, it is TiO_2's surface properties that determine its behavior and, hence, the surface has developed into a benchmark transition-metal oxide surface for studying many different processes.[4] The most stable (110) surface is characterized by rows of oxygen atoms bridging titanium ions (see Fig. 1). The basic physical and electronic structure of the surface has been well studied both experimentally[5,6] and theoretically,[7–11] and now many investigations focus on defected surfaces, especially oxygen vacancies,[12,13] adsorption,[14–17] or even adsorption onto defected surfaces.[18,19]

The tool of choice for studying such local processes on surfaces is scanning probe microscopy (SPM). Although in principle an insulator, TiO_2's small band gap (3 eV for the stoichiometric surface) means it is accessible to both scanning tunneling microscopy (STM) and noncontact atomic force microscopy (NC-AFM). Atomic resolution has been achieved on the (110) surface in both STM (Ref. 5) and NC-AFM.[20] For STM, the source of contrast in images was identified through extensive cooperation between theory and experiment, identifying Ti atoms [atom (4) in Fig. 1] as the tunneling sites.[5] In NC-AFM, theoretical interpretation is less well-developed and interpretation was found by combining STM and NC-AFM experimental studies of formic acid adsorption.[21,22] They found that the bridging oxygen site [atom (1) in Fig. 1] was seen as bright in their NC-AFM images. In both STM and NC-AFM interpretations, bridging oxygen vacancies were also used as markers to help in determining which sites were responsible for bright contrast.

An initial theoretical study of NC-AFM on TiO_2 (Ref. 23) calculated force curves over a few surface sites, and found that the largest force was over the bridging oxygen site. However, the authors used only a single hydrogen terminated silicon atom as a tip, and did not consider tip relaxation, finding they could not reconcile the very large contrast they found on the (1×1) surface in comparison to the (1×2) with experimental results.[24] Since the TiO_2 (110) surface remains a significant element in many fundamental surface studies, and continues to play a role in NC-AFM studies of surface defects and adsorption,[25] it is important to investigate in detail the NC-AFM tip-surface interaction for ideal and defected surfaces. In this work we use a combination of first-principles and atomistic simulations to study the interaction of several tip models with the ideal TiO_2 (110) surface, and the interaction of a silicon tip with an oxygen vacancy in the surface.

II. METHODS

A. Tip and surface setup

The central unknown in NC-AFM remains the microscopic nature of the tip, and as such, any attempt at simulation must take into account different possibilities. In most NC-AFM experiments[25] the, originally silicon, tip makes contact with the surface before scanning and is likely to be coated by surface material—in the case of the TiO_2 surface this can be expected to be in the form of an oxide layer. Even

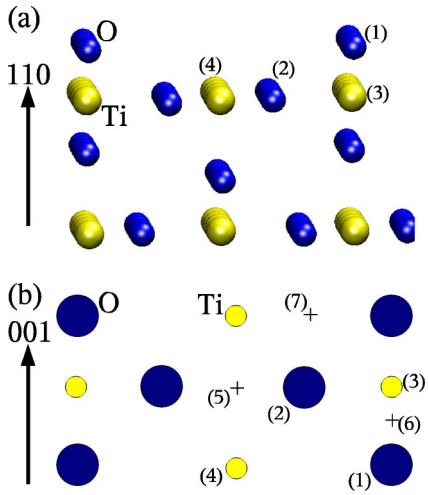

FIG. 1. Atomic structure of the TiO_2 (110) surface from (a) the side and (b) from the top. The labels are surface position references which are used throughout the text.

if contact is avoided, the tip will be oxidized without further treatment, although the possibility to tunnel through such tips into the TiO_2 surface[20] suggests this oxidation is not complete. Also, in some experiments on TiO_2 (Ref. 24) the tip has been cleaned by sputtering. This leaves two possibilities for the tip apex in NC-AFM on TiO_2: an oxide tip produced by contact with the surface or exposure to the environment; a clean silicon tip due to incomplete oxidation or cleaning treatment. In order to study both these tip models, we have considered two tip-surface systems and effectively three different tips in this work.

The oxide tip is modeled by a 64-atom MgO cube, orientated with the *z* axis parallel to the (111) direction of the unit cell. This cube can be orientated with either a single O or Mg atom at the lower apex, thereby providing either a net negative or positive electrostatic potential towards the surface. Previous simulations with this tip agree with experiments where tip contamination by ionic material is probable.[26] The oxide tip calculations were performed using atomistic simulations and the MARVIN2 code.[27,28] This technique uses point charges and polarizable shells to represent atoms, and pair potentials to represent atomic interactions. The pair potential parameters for the systems discussed in this work have been taken from previous publications on MgO (Ref. 29) and TiO_2.[30] Note here that we have used a mixture of partial and formal charges for the combined tip-surface system, however, we tested many parameter sets for TiO_2 and this was the only set that provided a reasonable model of the (110) surface, i.e., that actually gave a surface structure which was close to experiment after relaxation. For atomistic simulations, the TiO_2 (110) surface was represented by a $(6\times6\times3)$ slab, which provides surface relaxations in qualitative agreement with previous *ab initio* calculations[11] and experiments.[6] During simulations the top third of the tip and the bottom third of the surface were kept frozen, and all other ions were allowed to relax freely.

The pure silicon tip was represented by a ten-atom silicon cluster with a single dangling bond at the apex and its base terminated by hydrogen.[31,32] This tip is produced by taking three layers from the Si (111) surface and removing atoms to produce a sharp apex. Besides providing a fair model of the structure of the most stable Si (111) surface, it also provides the dangling bond characteristic of the most stable (7×7) reconstruction. However, the small size, specific shape, and hydrogen termination of the tip produce a surface electronic structure different from a standard silicon surface. The real test of this tip's validity is in comparison to experiment, where it has demonstrated excellent agreement when comparing forces over a silicon surface.[33] The silicon tip calculations were performed using the linear combination of atomic-orbitals basis SIESTA code,[34,35] implementing the density-functional theory with the generalized gradient approximation and the functional of Perdew, Burke, and Ernzerhof.[36] Core electrons are represented by norm-conserving pseudopotentials using the Troullier-Martins parametrization.[35] The pseudopotential for the silicon atom was generated in the electron configuration $[\mathrm{Ne}]3s^2\,3p^2$, oxygen in $[1s^2]2s^2\,2p^4$, and titanium in $[\mathrm{Ar}]4s^2\,3d^2$, where square brackets denote the core electron configurations. Various basis set configurations were tested, and a good compromise between accuracy and efficiency was found using double ζ with polarization for Ti, Si, and H, and using triple ζ with polarization for O. All calculations were converged to the order of meV in the total energy with respect to *k* points, mesh cutoff, and orbital cutoffs (i.e., energy shift[35]). Initial calculations on the surface itself were performed on a 36-atom $[(1\times1\times3)$ in terms of the six-atom surface unit cell] cell using 12 *k* points $(4\times4\times1$ *k*-point mesh), a mesh cutoff of 126 Ry, and an energy shift of 15 meV. We found that this gives surface relaxations in reasonable agreement with previous *ab initio* calculations[11] and experiments.[6] To check the dependence of our results on the slab thickness, we also calculated $(1\times1\times6)$ and $(1\times1\times7)$ slabs, and found that the surface relaxations have converged to less than 0.01 nm (and much better than this in most cases). This agrees with previous studies of TiO_2 surface slab thickness.[16,23]

For SIESTA calculations of the full tip-surface system, the TiO_2 (110) surface itself was modeled by a $(4\times2\times3)$ slab in terms of the six-atom surface unit cell, now using only the γ point. The much larger slab is required to avoid the spurious interactions between images of the tip. During simulations the top half of the tip and the bottom third of the surface were kept frozen, and all other ions were allowed to relax freely to less than 0.05 eV/Å. We did not consider a full spin-polarized treatment of the problem since previous studies using similar[23] and identical methods[32] indicate that it is not significant. Finally, it should be pointed out that although the first-principles and empirical methods are very different, calculations of the same tip-surface system with both methods provided good qualitative agreement, and a quantitative agreement to within 20% accuracy.[37]

B. Simulating NC-AFM

The complete tip-surface system has now been established and the method for calculating the microscopic tip-surface interaction discussed. This leaves only a model of the cantilever oscillations as the final part of the NC-AFM modeling process. In the standard mode of NC-AFM operation an image is produced by specifying a constant frequency change of the cantilever oscillations due to the tip-surface interaction. Then the deflection of the cantilever required to maintain this frequency change as the tip scans across the surface is measured as topographical contrast in an image. In this study we use the method described in Ref. 29 to model the oscillations, but other possibilities exist and are discussed in Ref. 25. In this method the cantilever is described by a simple equation of motion, defined by experimental oscillation parameters, and its behavior under the influence of the total tip-surface interaction is numerically calculated. An interpolation is then made at a given constant frequency change of the cantilever oscillations to find the tip height at every surface position and, hence, the simulated image.

The total tip-surface interaction here is a combination of the microscopic forces discussed above and a macroscopic background force due the van der Waals interaction of the macroscopic tip with the surface. The macroscopic tip is

TABLE I. Mean height and contrast for the three different tip models at various constant frequency changes. The distance is with reference to the equilibrium position of the bridging oxygen (1).

Δf	Mean distance (nm)			Contrast (nm)		
(Hz)	Si tip	O tip	Mg tip	Si tip	O tip	Mg tip
−80	0.32	0.45	0.46	0.070	0.069	0.071
−90	0.29	0.36	0.37	0.085	0.211	0.164
−100	0.27	0.31	0.30	0.107	0.173	0.283

modeled by a cone with a sphere at its apex,[29] and the van der Waals force is then dominated by the radius of the sphere. The ''tip'' radius is a parameter of the image simulations, and we fit it by making sure we get the same contrast seen in experiments for a given frequency change. This effectively corresponds to matching one point on a frequency change versus distance curve. Under the assumption that the background forces are dominated by the van der Waals force, this is a good approximation. The experimental oscillation parameters used in the simulations are: cantilever spring constant of 28 N/m, oscillation frequency of 270 kHz, and amplitude of 15 nm.[20] Experimental atomic resolution for those parameters was achieved at a constant frequency change (Δf) of −81 Hz with a contrast of 0.07 nm [this gives a normalized frequency shift $\gamma_0 = 15.0$ (Ref. 38)], which corresponds in simulations with the silicon tip to a macroscopic tip radius of 32.5 nm, and 57.5 nm radius for the oxide tip. In both cases we use a Hamaker constant of 0.6 eV,[39] which represents the interaction of SiO_2 with TiO_2 in vacuum at room temperature. We use SiO_2 for both since in the experiments we are modeling, the tip is not sputtered or heated to high temperatures, and on the macroscopic scale it will be oxidized regardless of the specific structure at the very end. The contrast and average tip-surface distance as a function of frequency change are summarized in Table I. It should be emphasized that this fitting allows direct comparison between experimental and theoretical images with the same oscillation parameters, but the real atomic interactions responsible for contrast remain as calculated in microscopic simulations.

III. THE STOICHIOMETRIC SURFACE

We first consider the stoichiometric TiO_2 (110) surface, and compare the tip-surface interactions and simulated images for the three different tip models. In the following discussion note that we are using a consistent reference for height, the equilibrium position of the bridging oxygen (1), and this means that the other atoms are about 0.1 nm further from the tip. However, it is important to emphasize that the tip interacts with the whole surface, not just the single atom directly under the apex and artificially shifting the force curves would be misleading. Figure 2(a) shows the microscopic forces over different surface sites for the silicon tip. We see immediately that the force is dominated by the interaction of the tip with the bridging oxygen sites: the largest forces are over positions (1)—directly over the bridging oxygen, (3)—at the midpoint of two bridging oxygens over Ti,

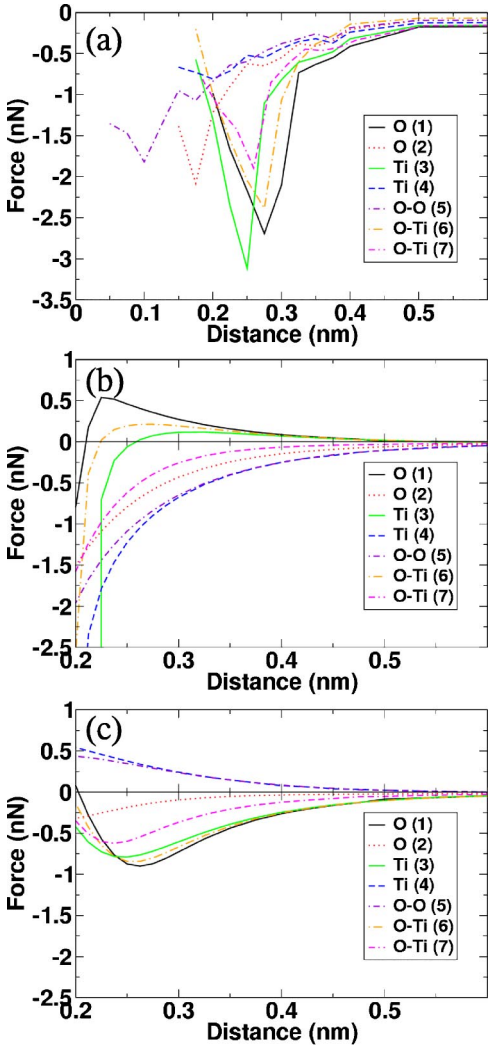

FIG. 2. Tip-surface forces over various sites in the TiO_2 (110) surface for the three different tip models considered in this study: (a) silicon tip, (b) oxide tip with oxygen at the apex, and (c) oxide tip with magnesium at the apex. The numerical labels in the legends refer to Fig. 1 and the distance is with reference to the equilibrium position of the bridging oxygen (1).

and (6) and (7)—at midpoints from the bridging oxygen to Ti sites. The absolute maximum occurs over position (3), with a force of over 3 nN at 0.25 nm, but the force over position (1) dominates the curves from 0.50 to 0.25 nm. Displacement of atoms also plays a role in the interaction, with the bridging oxygen displaced out from the surface by 0.02 nm and the tip apex 0.01 nm displaced towards the surface at a distance of 0.3 nm when the tip is at site (1). If we now look at the electronic structure of the tip and surface at maximum force (only possible for the SIESTA calculations) we see that the interaction is dominated by the onset of covalent bonding between the tip apex and the atoms in the surface. Over the O(1) site a clear bond can be seen in the charge density between the tip and surface, and analysis of charge transfer shows that over 0.4 electrons have transferred between the tip and surface.[37] When the tip is at 2.5 nm over site (3), at the absolute force maximum, bonds can be seen between both bridging oxygen atoms and the tip. Over the Ti(4) site

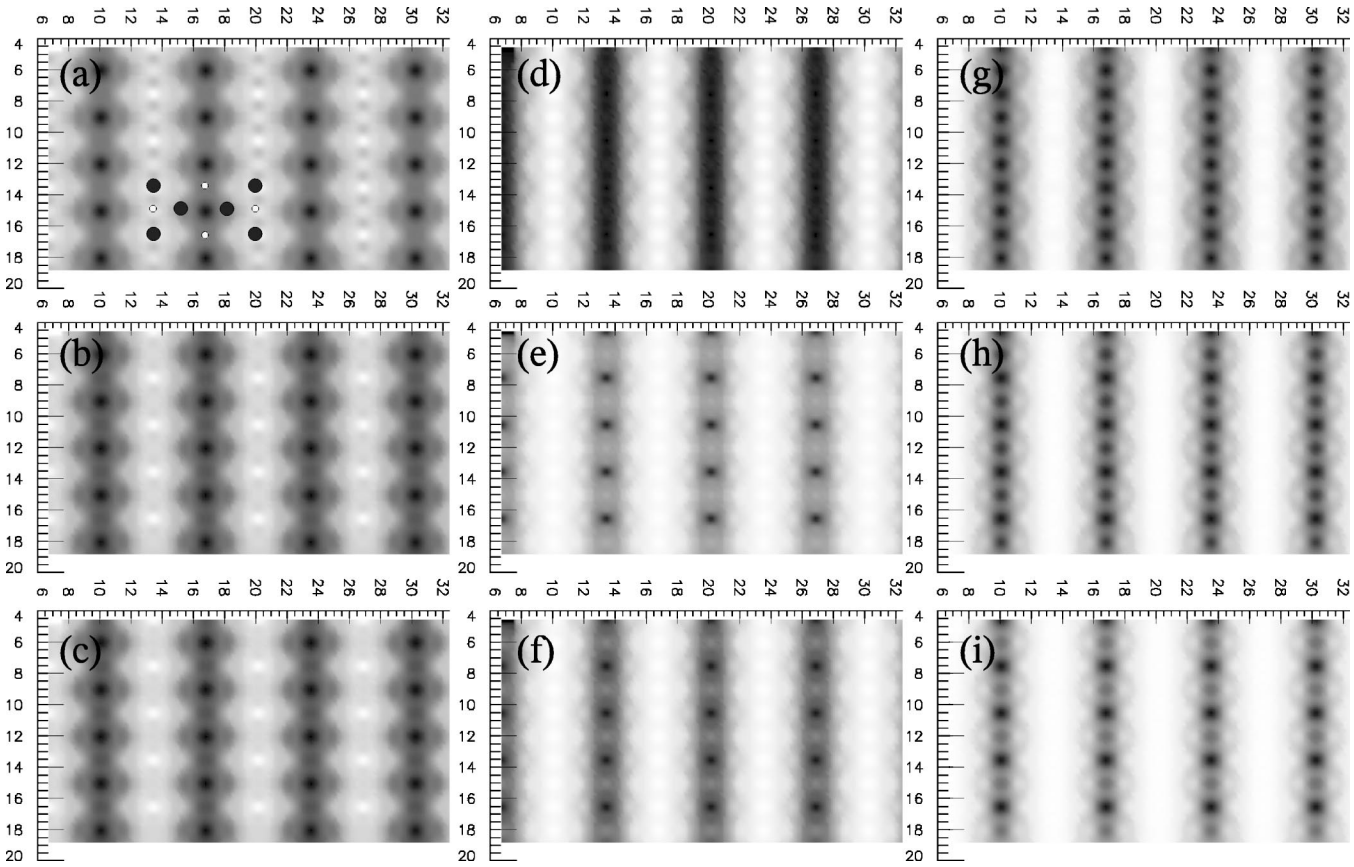

FIG. 3. Simulated NC-AFM images of the TiO_2 (110) surface with a silicon tip (a–c), an oxide tip with oxygen at the apex (d–f), and an oxide tip with magnesium at the apex (g–i). The images were calculated at constant frequency changes of -80 Hz (a,d,g), -90 Hz (b,e,h), and -100 Hz (c,f,i). Image (a) contains a version of Fig. 1(b) to show the atomic structure orientation.

no bond can be seen, and any charge transfer is with the surrounding oxygen ions. This behavior is consistent for other insulating surfaces interacting with a silicon tip, where force is always dominated by the interaction with anions in the surface.[37] Following this, we also calculated a force curve over a site midway between sites (2) and (3) (not shown in Fig. 2). Since this point is actually at the center of three oxygen atoms, we were interested in whether the force maybe even larger than that over site (3). However, the fact that one of the oxygens [at site (2)] is much lower, and the tip is further from the bridging oxygens, meant the force is much smaller than that over site (3).

If we now compare these results with previous calculations,[23] we see that using a more realistic tip and including tip relaxation results in a reduction in the maximum force over O(1) by over a factor of 2. We also see that the position of this maximum shifts by 0.05 nm outward from the surface. As suggested by the Ke *et al.*,[23] the very idealistic single-atom tip they use is probably responsible for the disagreement between experiment and theory in the relative magnitude of contrast for the (1×1) and (1×2) surfaces. The contrast on the (1×1) surface is mainly due to the difference in force over O(1) and Ti(4). Since tip relaxation is not a large factor for the Ti site, a small frozen tip is a better approximation, but over O(1), relaxation is significant and a frozen tip greatly exaggerates the force—and hence the contrast on the surface.

This dominance of the bridging oxygen interaction translates directly into the bright rows seen in Figs. 3(a)–3(c), where atomic resolution is almost lost and the bridging oxygen rows just appear as bright stripes. As the frequency change of the image is increased through Figs. 3(a)–3(c), the imaging height is reduced and the relative dominance of the bridging oxygen increases, making the rows brighter. Even though the absolute force maximum occurs over Ti(3), if we go closer it is still not possible to generate an image with a contrast maximum at that site, as the required frequency change cannot be produced over the other sites. Finally, we point out that the image shown in Fig. 3(a) is produced using identical parameters, including contrast, as that shown in experiments on TiO_2 (Ref. 20) and we see that the simulated image contrast pattern is in very good agreement with the experimental one.

Figure 2(b) shows force curves over the same sites, but now with the oxygen-terminated oxide tip. The source of contrast is now reversed, with the strong attraction between the positive Ti ions in the surface and negative electrostatic potential from the tip dominating the interaction. We also see that in general the force magnitude is smaller than that for the silicon tip. The atomic displacements are correspondingly much smaller—Ti (4) is displaced towards the tip by only 0.001 nm at 0.3 nm, and the tip atoms do not displace at all. Only at close range, less than 0.2 nm, do we see larger forces, but this is due to large jumps of surface ions to the tip

and these will result in abrupt contrast changes or tip crashes in experiments. The jumps also prevent the tip reaching the pure maximum force, and the force increases smoothly until a jump point is reached. Over sites (1), (2), and (3), the ''bridging oxygen sites,'' we actually see an overall repulsion between the negative potential tip and negative O ions in the surface. This repulsive interaction [seen also in Fig. 2(c)] is actually responsible for the greatly increased macroscopic tip radius required for the oxide tip to achieve experimental contrast at experimental frequency changes. NC-AFM by design can only operate in an overall attractive regime, so this repulsive component must be compensated by attractive van der Waals forces—without it, the tip-surface interaction over these sites will never be attractive enough to produce a frequency change of -80 Hz. For the silicon tip, there is no repulsive component and the background van der Waals force needed to match experimental contrast is much smaller. The images [Figs. 3(d)–3(f)] produced with the oxygen-terminated oxide tip demonstrate even more vivid stripe patterning, with contrast detail between the Ti rows appearing only at closer separation in Fig. 3(e). At a frequency change of -100 Hz we actually see the contrast reduce (see Table I) due to the onset of jumps in the force, see, for example, the force curve over site (3) at 0.22 nm in Fig. 2(b).

For the final tip model, the positively terminated oxide tip, we see almost opposite behavior to that for the negatively terminated tip—as one would expect. The force curves in Fig. 2(c) are now dominated by interaction with the bridging oxygen and nearby sites. The force curves are now slightly smoother than that for the O-terminated tip, and we do not see any jumps until below 0.2 nm, hence the contrast also increases uniformly as we approach the surface (see Table I). At 0.3 nm, the bridging oxygen is displaced towards the tip by 0.005 nm, and the tip atoms do not show significant displacements. Simulated images with this tip [Figs. 3(g)–3(i)] once again show bright stripes along the bridging oxygen rows, as for the silicon tip.

Note that for all three tip models, the contrast pattern agrees qualitatively with experiment, and without an external source of further information it would be difficult to establish which sublattice is really seen in experiments. As discussed previously, a combination of NC-AFM, STM, and adsorption studies strongly suggest that, at least in those experiments,[20–22] the bridging oxygen rows were imaged as bright. The fact that the experiments were able to obtain a tunneling signal effectively excludes a strongly ionic tip, and suggests that the silicon model is more appropriate. However, we cannot exclude a conducting tip with, for example, a single positive ion, such as titanium, at the apex. As the calculations have shown, both these cases would provide images in agreement with experimental results.

One further interaction which could be considered when dealing with a conducting tip and an insulating surface is the image force.[40] This contribution is due to the polarization of conducting materials, i.e., polarization of the tip due to charged atoms in the sample, and it is only really significant for a very conducting tip such as a metal or heavily doped silicon. When introduced for calculations on TiO_2, the position of the bridging oxygens above the surface means that there is no compensation from an oppositely charged ion at the same height, as there is for the titanium ions in the surface.[41] This uncompensated interaction produces a strong image force, and would dominate contrast.[41] If such tip control was possible, it would be very interesting to compare imaging with clean metallic and oxidized silicon tips systematically to study the possible role of image forces.

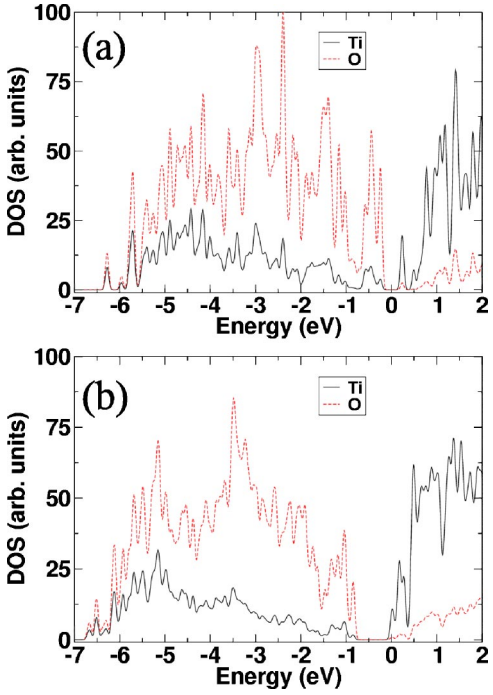

FIG. 4. Calculated partial density of states for (a) the stoichiometric TiO_2 surface and (b) the surface with an oxygen vacancy. The energy scale has been corrected so that the Fermi energy is at 0 eV. Gaussian broadening with width 0.05 eV was applied to the results.

IV. DEFECTED SURFACE

In order to also study the interaction of the tip with a defected surface, we have investigated the TiO_2 (110) surface with one bridging oxygen (1) atom removed. Previous calculations on the reduced surface[10,12,42] demonstrated some spread in electronic structure predictions for this system, although general features remained similar. Here we use the recent combined full potential linearized augmented plane-wave calculations and experiments in Ref. 42 as a reference. In that work, the authors found that removal of the bridging oxygen atoms introduces an occupied state at the edge of the conduction band with Ti character. Examination of the density of states, shown in Figs. 4(a) and 4(b), shows that we find exactly the same behavior. For the ideal surface, we see that the valence band is dominated by O *p* states and the conduction band by Ti *d* states. Note that the conduction-band edge appears as a rather discrete Ti state due to the small Fermi smearing used in the calculations and small energy window shown—it is not a defect/surface state, but represents the beginning of the conduction band. After removing the oxygen atom, the two electrons originally localized on

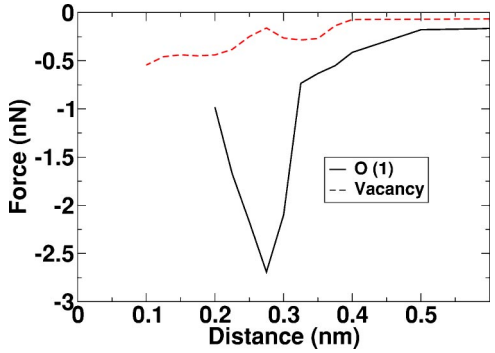

FIG. 5. Comparison of the force over a bridging oxygen O(1) site and a bridging oxygen vacancy.

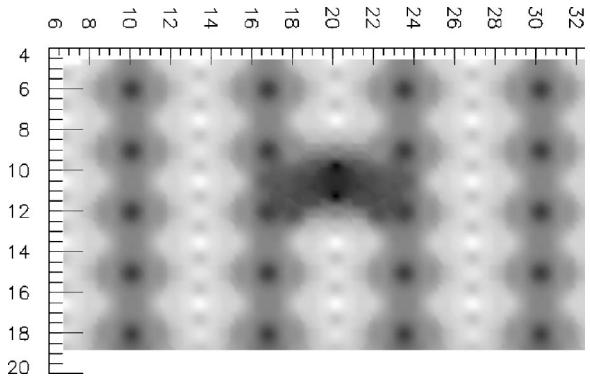

FIG. 6. Simulated image of the defected surface calculated at a frequency change of −80 Hz with a silicon tip. The bridging oxygen vacancy is at about (20.2,10.5) in the image.

the oxygen do not remain in the vacancy, but go to unoccupied *d* states of Ti, and the Fermi energy intersects a state at the edge of the conduction band [Fig. 4(b)]. As in Refs. 10,12 we find that the spin-polarized defected surface is energetically favorable (by 0.13 eV in our case) but that this does not make a significant difference to the surface geometry or the nature of the vacancy itself. Since we are interested primarily in the tip-surface force over the vacancy site, further calculations were restricted to spin-paired ground states.

The preceding section demonstrated that the silicon tip model gives good agreement with experiment, hence for the vacancy the setup and calculation method is exactly the same as for the previous silicon tip simulations, but with one oxygen atom removed from the surface. Figure 5 shows a comparison of the force over site (1) with and without the bridging oxygen atom present. We see immediately that the force over the vacancy is much smaller than that over the bridging oxygen, in fact, the force over the vacancy is smaller than the force over any of the atomic sites shown in Fig. 2(a). This is a consequence of the nature of the vacancy in TiO_2. Unlike in other more ionic materials such as MgO,[43] no electrons remain in the vacancy and the vacancy basically increases the distance of the tip apex from any surface ion compared to the ideal surface. As the tip gets closer, the force rises [although it is still much less than that over O(1)] due to interactions between the apex and atoms below the vacancy, and also between the sides of the tip and atoms in the surface. However, this is at distances of less than 0.2 nm and the large repulsion felt over other atomic sites at such small tip-surface separations means that it would be impossible to image in NC-AFM. Hence, we can conclude, as shown in Fig. 6, that oxygen vacancies in the TiO_2 (110) surface would appear as areas of very weak interaction, i.e., dark contrast, on the bright contrast rows of bridging oxygen atoms. Note that the basically geometrical nature of the reduction in contrast over vacancies means it should be consistent for any tip structure.

V. DISCUSSION

For the ideal TiO_2 (110) surface, we have shown that, in principle, qualitative agreement with NC-AFM images can be achieved for simulations with three different tip models. This means, as shown for other insulators,[26] that simple intuitions based on surface geometry can be very misleading. Information from combined STM and NC-AFM experimental studies of adsorption on TiO_2 suggest that the bridging oxygen rows are imaged as bright in most studies, and the theoretical results presented here using a silicon tip or a positive potential oxide tip and experimental imaging parameters agree with this result. By using a large silicon tip and allowing tip relaxation, we obtain a maximum force over the TiO_2 surface which is half that seen in previous calculations.[23] The overestimation of the force is likely to explain the earlier predicted reversal of relative contrast on the (1×1) and (1×2) surfaces with respect to experiment.[24]

Calculations for the bridging oxygen vacancies establish clearly that they would appear as dark in images where the bridging oxygen rows appear bright—supporting the previous intuition from experiment.[20] This means vacancies can be used as chemical markers in NC-AFM experiments, in a similar way to their use in STM.[5] Since their presence in the surface can be controlled by annealing in either an oxygen atmosphere or vacuum, increasing their concentration should indicate the bridging oxygen rows and hence make it much easier to understand other processes on the surface, such as adsorption or diffusion.

The future development of NC-AFM as a reliable surface science tool depends rather heavily on providing a more systematic interpretation system. In this work we find, once again,[25] that the greatest difficulties arise from the lack of information about the tip. Although we can infer certain properties indirectly, e.g., through the tunneling signal, much greater success would be achieved if the tip could be controlled. It has been shown that a pure silicon tip would provide a consistent basis for interpretation,[37] and advances in routine preparation of such a tip would greatly aid the field.

It is also interesting to note the predicted increase in tip radius required to provide the same contrast with an oxide tip as for a silicon tip. The increased van der Waals force basically compensates for the repulsive component of the oxide tip interaction, allowing one to go closer while still having an overall attractive force—the condition for stable NC-AFM

operation. Without compensation the stable operating range where measurable contrast is possible is reduced, and atomic resolution would be more difficult. This need to compensate for the repulsive component of the interaction may explain the common (and poorly understood) practice of contacting the surface before successfully achieving atomic resolution. Contact can reduce this repulsive component in several, nonexclusive ways: (i) the initially sharp tip is blunted increasing the radius and the van der Waals force, (ii) the tip is coated by surface material changing the Hamaker constant and again increasing van der Waals force, and (iii) contact changes the structure of the end of the tip making it less polar. Recent experimentally obtained site specific force curves on insulators do not show a repulsive component over any atoms after removing background forces,[44–46] supporting this assertion. Again this aspect of NC-AFM should be unnecessary if the tip structure were controlled during experiments.

ACKNOWLEDGMENTS

This research was supported by the Academy of Finland through its Center of Excellence Program (2000–2005). We are grateful to Y. -J. Lee for useful discussions, and to the Center of Scientific Computing (CSC), Helsinki, for computational resources. We wish to thank A. L. Shluger for critical comments on the manuscript.

*Electronic address: asf@fyslab.hut.fi; www.fyslab.hut.fi/~asf/physics/Physics.html

[1] A.L. Linsebigler, G. Lu, and J.T. Yates, Chem. Rev. (Washington, D.C.) **95**, 735 (1995).
[2] V. E. Henrich and P. A. Cox, *The Surface Science of Metal Oxides* (University Press, Cambridge, 1996).
[3] J. Lausmaa, J. Electron Spectrosc. Relat. Phenom. **81**, 343 (1996).
[4] U. Diebold, Surf. Sci. Rep. **48**, 53 (2003).
[5] U. Diebold, J.F. Anderson, K.O. Ng, and D. Vanderbilt, Phys. Rev. Lett. **77**, 1322 (1996).
[6] G. Charlton *et al.*, Phys. Rev. Lett. **78**, 495 (1997).
[7] D. Vogtenhuber, R. Podloucky, A. Neckel, S.G. Steinemann, and A.J. Freeman, Phys. Rev. B **49**, 2099 (1994).
[8] M. Ramamoorthy, R.D. King-Smith, and D. Vanderbilt, Phys. Rev. B **49**, 7709 (1994).
[9] M. Ramamoorthy, D. Vanderbilt, and R.D. King-Smith, Phys. Rev. B **49**, 16 721 (1994).
[10] P.J.D. Lindan, N.M. Harrison, M.J. Gillan, and J.A. White, Phys. Rev. B **55**, 15 919 (1997).
[11] N.M. Harrison, X.G. Wang, J. Muscat, and M. Scheffler, Faraday Discuss. **114**, 305 (1999).
[12] A.T. Paxton and L. Thiên-Nga, Phys. Rev. B **57**, 1579 (1998).
[13] R. Schaub, E. Wahlström, X. Rønnau, E. Lægsgaard, E. Stensgaard, and F. Besenbacher, Science **299**, 377 (2003).
[14] S.P. Bates, G. Kresse, and M.J. Gillan, Surf. Sci. **409**, 336 (1998).
[15] P.J.D. Lindan, N.M. Harrison, and M.J. Gillan, Phys. Rev. Lett. **80**, 762 (1998).
[16] J. Muscat, N.M. Harrison, and G. Thornton, Phys. Rev. B **59**, 2320 (1999).
[17] I.M. Brookes, C.A. Muryn, and G. Thornton, Phys. Rev. Lett. **87**, 266103 (2001).
[18] G. Liu, J.A. Rodriguez, Z. Chang, J. Hrbek, and L. González, J. Phys. Chem. B **106**, 9883 (2002).
[19] E. Wahlström, N. Lopez, R. Schaub, P. Thostrup, A. Rønnau, C. Africh, E. Lægsgaard, J.K. Nørskov, and F. Besenbacher, Phys. Rev. Lett. **90**, 026101 (2003).
[20] K.I. Fukui, H. Onishi, and Y. Iwasawa, Phys. Rev. Lett. **79**, 4202 (1997).
[21] K.I. Fukui, H. Onishi, and Y. Iwasawa, Chem. Phys. Lett. **280**, 296 (1997).
[22] Y. Iwasawa, Surf. Sci. **402-404**, 8 (1998).
[23] S.H. Ke, T. Uda, and K. Terakura, Phys. Rev. B **65**, 125417 (2002).
[24] M. Ashino, Y. Sugawara, S. Morita, and M. Ishikawa, Phys. Rev. Lett. **86**, 4334 (2001).
[25] *Noncontact Atomic Force Microscopy,* edited by S. Morita, R. Wiesendanger, and E. Meyer (Springer, Berlin, 2002).
[26] A.S. Foster, C. Barth, A.L. Shluger, R.M. Nieminen, and M. Reichling, Phys. Rev. B **66**, 235417 (2002).
[27] D.H. Gay and A.L. Rohl, J. Chem. Soc., Faraday Trans. **91**, 925 (1995).
[28] A.L. Shluger, A.L. Rohl, D.H. Gay, and R.T. Williams, J. Phys.: Condens. Matter **6**, 1825 (1994).
[29] A.I. Livshits, A.L. Shluger, A.L. Rohl, and A.S. Foster, Phys. Rev. B **59**, 2436 (1999).
[30] M. Matsui and M. Akaogi, Mol. Simul. **6**, 239 (1991).
[31] R. Pérez, I. Stich, M.C. Payne, and K. Terakura, Phys. Rev. B **58**, 10 835 (1998).
[32] A.S. Foster, A.Y. Gal, Y.J. Lee, A.L. Shluger, and R.M. Nieminen, Appl. Surf. Sci. **210**, 146 (2003).
[33] M.A. Lantz, H.J. Hug, P.J.A. van Schendel, R. Hoffmann, S. Martin, A. Baratoff, A. Abdurixit, H.J. Güntherodt, and C. Gerber, Phys. Rev. Lett. **84**, 2642 (2000).
[34] J. Junquera, O. Paz, D. Sánchez-Portal, and E. Artacho, Phys. Rev. B **64**, 235111 (2001).
[35] J.M. Soler, E. Artacho, J.D. Gale, A. García, J. Junquera, P. Ordejón, and D. Sánchez-Portal, J. Phys.: Condens. Matter **14**, 2745 (2002).
[36] J.P. Perdew, K. Burke, and M. Ernzerhof, Phys. Rev. Lett. **77**, 3865 (1996).
[37] A. S. Foster, A. Y. Gal, J. M. Airaksinen, O. H. Pakarinen, Y. J. Lee, J. D. Gale, A. L. Shluger, and R. M. Nieminen, Phys. Rev. B (to be published).
[38] F.J. Giessibl, Phys. Rev. B **56**, 16 010 (1997).
[39] L. Bergström, Adv. Colloid Interface Sci. **70**, 125 (1997).
[40] L.N. Kantorovich, A.S. Foster, A.L. Shluger, and A.M. Stoneham, Surf. Sci. **445**, 283 (2000).
[41] A. S. Foster, Ph.D. thesis, University College London, 2000 (unpublished); see also http://www.fyslab.hut.fi/asf/physics/thesis1/thesis1.html.

[42] D. Vogtenhuber, R. Podloucky, J. Redinger, E.L.D. Hebenstreit, W. Hebenstreit, and U. Diebold, Phys. Rev. B **65**, 125411 (2002).
[43] G. Pacchioni, A.M. Ferrari, and G. Ieranò, Faraday Discuss. **106**, 155 (1997).
[44] R. Hoffmann, M.A. Lantz, H.J. Hug, P.J.A. van Schendel, P. Kappenberger, S. Martin, A. Baratoff, and H.J. Güntherodt, Appl. Surf. Sci. **188**, 238 (2002).
[45] R. Hoffmann, L. N. Kantorovich, A. Baratoff, H. J. Hug, and H. J. Güntherodt (unpublished).
[46] S.M. Langkat, H. Hölscher, A. Schwarz, and R. Wiesendanger, Surf. Sci. **527**, 12 (2003).